Modeling and Multi-objective Optimization of Carbon Emissions Throughout the Lifecycle of Zero Carbon Buildings

Xueli Yin*, Yingrui Dong, Luyao Pei and Rong Hu

Energy Development Research Institute, CSG, Guangzhou 510530, Guangdong, China
E-mail: xueliyin_res@126.com
**Corresponding Author*

Received 09 December 2025; Accepted 07 January 2026

Abstract

To manage the carbon emissions of zero carbon buildings, a building information model is used to construct a carbon emission model for zero carbon buildings, and a multi-objective optimization method based on non dominated genetic algorithm is developed to optimize the carbon emissions. The performance of the carbon emission model is analyzed using the China Energy and Carbon Emission Database (MEIC) public database, and the outcomes reveal that the data matching error rate of the model is less than 5%, and the model's coverage of the whole span of carbon emissions reaches 87.9%. By reusing the data from Global Carbon Budget (GCB) database to predict the carbon reduction effect of the optimization plan, the outcomes reveal that the optimization plan can reduce the carbon emissions throughout the whole span by 35% to 45%, and the carbon reduction during the operation phase can reach 43.7%. From the above outcomes, the emission

Strategic Planning for Energy and the Environment, Vol. 45_2, 375–402.
doi: 10.13052/spee1048-5236.4524

reduction plan based on carbon emission model and multi-objective optimization method can effectively reduce the carbon emissions. This can foster sustainable development, and provide ideas for carbon reduction plans in other fields.

Keywords: Decarbonization and emission reduction, carbon emissions, non-dominated genetic algorithm, building information modeling, multi-objective optimization.

Introduction

The issue of carbon emissions (CEs) has garnered worldwide attention due to global climate change, and carbon reduction is urgently needed [1]. However, in the realm of building CE management, traditional methods are often limited to single stage or single factor control, lacking systematic consideration of the whole span of buildings [2]. In the field of architecture, zero carbon buildings usually refer to buildings that achieve zero net carbon emissions throughout their entire lifecycle through comprehensive measures such as energy-saving design, renewable energy utilization, and carbon offset mechanisms [3]. According to internationally recognized standards, the accounting for zero carbon buildings should include the following boundaries. Time boundary: covering the entire life cycle of a building, including the production and transportation of building materials, construction, operation and maintenance, and demolition and recycling stages; Space boundary: including the building itself and its associated energy systems, as well as indirect emissions such as transportation and waste disposal. Carbon offset mechanism: allows offsetting the remaining carbon emissions that cannot be reduced through technological means by purchasing nationally certified voluntary emission reductions (CCERs), green electricity certificates, or investing in carbon sequestration projects. The research by Wang G et al. showed that CEs throughout the building process were relatively concentrated and intense, which validated the importance of full lifecycle management [4]. Roijen E V et al. found that achieving net-zero greenhouse gas emissions might not only require reducing emissions but also the deployment of carbon dioxide (CO_2) removal technologies. This explored the potential of storing carbon dioxide in building materials each year. The research found that in new infrastructure, completely replacing traditional building materials with carbon dioxide storage alternatives could store up to 16.6 ± 2.8 billion tons of carbon dioxide annually. In addition, the carbon storage pool for building

materials will increase proportionally to the demand for these materials, which may reduce the need for geological, terrestrial or Marine storage that is more costly or poses higher environmental risks [5]. This study quantitatively analyzes the distribution of carbon emissions throughout the entire life cycle of buildings, using industrial and civil buildings as samples. The statistics show that the carbon emissions during the construction phase account for 40%–60% of the total emissions throughout the life cycle, and the emission intensity is 2–3 times that of the operation phase. Its core contribution lies in the empirical verification of the concentration and intensity of carbon emissions during the construction phase, directly supporting the importance of full lifecycle management. Building Information Modeling (BIM), as an integrated technology platform, can integrate data information from various stages of project planning, design, construction, and operation, providing comprehensive and accurate data support for CE management. Liu J et al. used system dynamics combined with multi-objective optimization (MOO) methods to effectively forecast the effects of various energy consumption modes on the future energy structure [6]. Mullen D et al. found that zero-carbon hydrogen from steam methane reforming (SMR) was too expensive, and the cost of carbon dioxide capture increased exponential as the remaining emissions approached zero. It was found that through the long-term price estimation of natural gas usage and DACCS, as well as the long-term price estimation of electrolytic hydrogen production, the cost of avoiding carbon dioxide from the fuel shift from natural gas to hydrogen was prospected [7]. This study adopts a coupling method of system dynamics and MOO to construct a system dynamics model of energy consumption, carbon emissions, and economic costs in Shandong Province as a case study. The MOO algorithm is used to predict the impact of different energy consumption modes such as coal power reduction, wind power and photovoltaic increment on the energy structure in 2030. Its core contribution lies in verifying the effectiveness of multi-objective optimization methods in energy structure optimization, but the research object is regional energy systems, which are not adapted to the multi-objective coupling scenarios of building carbon emissions, construction period, and cost. To achieve systematic management and optimization of carbon emissions throughout the entire life cycle of zero-carbon buildings, this research follows a closed-loop research process of "modeling $\rightarrow$ verification $\rightarrow$ optimization $\rightarrow$ prediction of emission reduction effects". Specifically as follows: (1) Modeling stage: Based on BIM technology, integrate the data of the entire life cycle of buildings to construct a dynamic calculation model for carbon emissions; (2) Verification stage:

Use the MEIC database to verify the accuracy of the model and evaluate the error rate and coverage rate; (3) Optimization stage: The improved NSGA-II algorithm is adopted to conduct multi-objective collaborative optimization of carbon emissions, construction period and cost; (4) Effect prediction stage: Simulate the emission reduction potential under different energy scenarios in combination with the GCB database, and evaluate the carbon emission reduction effect of the optimization plan. Compared with the existing methods, this research approach has constructed a BIM-based dynamic coupling model for carbon emissions throughout the entire life cycle, breaking through the disconnection between design and carbon emission calculation in traditional modeling and achieving data integration from design, construction to operation and demolition. Meanwhile, a three-layer progressive coding mechanism for the construction process of buildings was proposed, and the coding logic of the NSGA-II algorithm in the building scheduling problem was improved, making the optimization results have both theoretical optimality and engineering feasibility. In addition, a dual-database collaborative verification system of MEIC and GCB has been established. The former is used for model accuracy verification, while the latter is used for multi-scenario emission reduction prediction, enhancing the credibility and cross-scenario applicability of the model. The innovation of the research is mainly reflected in the following three aspects: (1) A three-layer progressive coding logic was proposed, and an automatic data exchange mechanism between the BIM model and the NSGA-II algorithm was constructed, achieving a closed-loop flow of data throughout the entire life cycle. Specifically, the first layer of coding determines the priority of construction activities, the second layer of coding selects construction plans for each activity, and the third layer of coding allocates corresponding resources. This coding method enables NSGA-II to synchronously adjust the construction sequence, process plan and resource combination during the optimization process, thereby achieving collaborative optimization among carbon emissions, construction period and cost. (2) The model was verified and the emission reduction effect was predicted by using the dual public databases of MEIC and GCB, which enhanced the reliability and applicability of the model.

1 Building Decarbonization and Emission Reduction Method Based on BIM and NSGA-II

The research uses the BIM technology to analyze the CEs of buildings throughout their whole span, and to model and calculate the CEs throughout

the building process. Based on this analysis, it develops a calculation plugin for CEs throughout the building process using programming software. Finally, the NSGA-II algorithm is used for MOO of decarbonization and emission reduction in zero carbon buildings.

1.1 Modeling Method for CEs of Zero Carbon Buildings Based on BIM Technology

To accomplish the objective of zero carbon buildings, it is necessary to effectively assess and reduce their CEs throughout their whole span. However, traditional CE modeling methods mostly rely on manual calculations and simplified models, often neglecting the comprehensive consideration of various aspects in the design, construction, operation, and decommissioning stages of buildings [8]. The information data contained in BIM models can run through the whole span of buildings, and therefore are often used as the basis for building construction management and operation maintenance [9]. To clarify the accounting scope of the research object, the accounting boundary of zero carbon buildings will be set as follows in this study. Implied carbon: carbon emissions covering stages such as building material production, transportation, and on-site construction; Operating carbon: including energy related emissions from building heating, cooling, lighting, equipment operation, etc; Demolition and carbon recycling: covering emissions from building demolition, waste disposal, and material recycling processes; Carbon offset and green electricity substitution: Allow offsetting some emissions through purchasing CCERs, green electricity, and other means. Based on this, research is being conducted to integrate CE data from various stages of buildings using BIM technology. The full lifecycle CE analysis process grounded in BIM technology is presented in Figure 1.

From Figure 1, the modeling process grounded in BIM technology covers building environment information, usage requirements, and other data. After completing the design optimization of building building functional requirements, structural layout, and CE benefits, the BIM model is created. The BIM model will be further analyzed according to the construction requirements. Throughout the building process, the building model will undergo real-time modifications grounded in the actual building entity to ensure consistency between the model and the actual building. After entering the operational phase, the BIM model continues to simulate management and optimize CEs during the building operation process. Ultimately, with the end of the building's lifecycle, BIM models guide the demolition work. Therefore, BIM

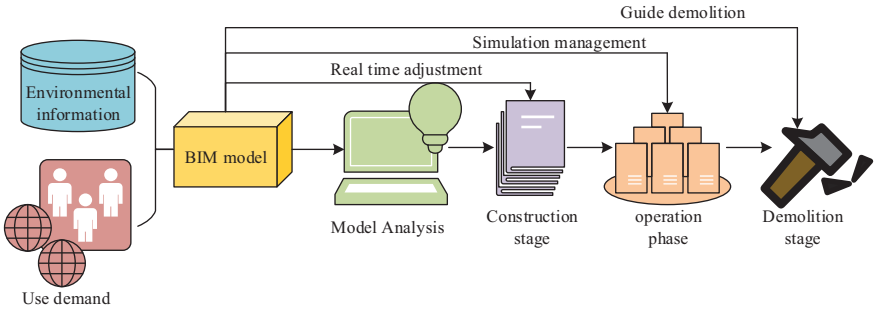

Figure 1 The whole span CE analysis process grounded in BIM technology.

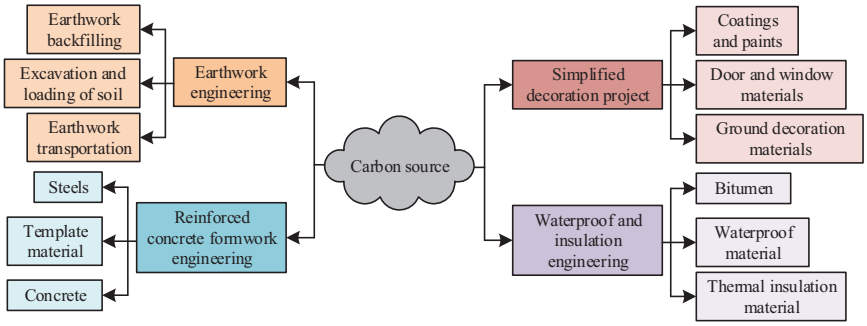

Figure 2 Factors affecting CEs throughout the building process.

models can provide simulation analysis data for the whole span of building structures. Throughout the whole span, CEs throughout the building process are relatively concentrated and intense [10]. Therefore, research is needed to establish a CE calculation platform based on BIM models throughout the building process, to achieve quantitative analysis of CEs during that phase.

To quantitatively analyze the CEs throughout the building process of buildings, a CE modeling of zero carbon buildings is studied based on the basic concept of CEs. The factors affecting CEs throughout the building process are presented in Figure 2.

In Figure 2, the construction of building buildings involves a large number of civil engineering projects, in which building materials such as steel, concrete, doors and windows, and coatings are used, accounting for 99% of the total CEs [11]. Therefore, to improve computational efficiency, the study only considers projects and related building materials with a high proportion of CEs as CE sources for detailed analysis. For projects and materials with low CEs throughout the building process, detailed calculations will not be

conducted. The mathematical model for calculating CEs is presented in Equation (1).

$$\min E = \sum_{i=1}^{n} \sum_{j=1}^{m} C_r^{ij} \tag{1}$$

In Equation (1), E is the total CEs throughout the building process of the building, and C_r^{ij} is the CEs of the jth project in the ith construction scheme. The computation of the CEs of each project is presented in Equation (2).

$$C_r^{ij} = Q_r^{ij} \times F_r^{ij} \tag{2}$$

In Equation (2), Q_r^{ij} and F_r^{ij} represent the engineering quantity and composite CEs under this scheme. The mathematical expression for composite CEs is presented in Equation (3).

$$F_r^{ij} = M_r^{ij} + R_r^{ij} + E_r^{ij} \tag{3}$$

In Equation (3), M_r^{ij}, R_r^{ij}, and E_r^{ij} represent the CEs released by materials, labor, and machinery for the jth project in the ith construction scheme. The computation for material CEs is presented in Equation (4).

$$M_r^{ij} = \sum_{x=1}^{a} M_r^{ix} \times E_x' \tag{4}$$

In Equation (4), M_r^{ix} is the consumption of the material used in this scheme, x is the total quantity of materials, and a is the CE factor under this material. The computation for artificial CEs is presented in Equation (5).

$$R_r^{ij} = \sum_{y=1}^{b} R_r^{iy} \times E_y' \tag{5}$$

In Equation (5), R_r^{iy} is the consumption of the yth type of worker under the rth construction scheme in the ith project, b is the total amount of workers, and E_y' is the CE factor of the yth type of worker. The computation for mechanical CEs is presented in Equation (6).

$$E_r^{ij} = \sum_{z=1}^{c} E_r^{iz} \times E_z' \tag{6}$$

In Equation (6), E_r^{iz} is the consumption of the type of machinery used in this scheme, z is the total amount of machinery, and c is the CE factor of the type of machinery.

1.2 Zero Carbon Building Decarbonization and Emission Reduction Design Based on MOO

Based on the modeling of CEs throughout the whole span of zero carbon buildings, to achieve a balance between cost, schedule, and CEs, MOO theory is used to solve the constructed mathematical model. MOO theory is a mathematical method that studies how to find the best compromise between multiple potentially conflicting objectives. Among numerous MOO algorithms, NSGA-II has high optimization accuracy [12, 13]. Therefore, the study utilizes the NSGA-II algorithm for MOO of decarbonization and emission reduction in zero carbon buildings. The coding of decarbonization and emission reduction design for buildings based on NSGA-II algorithm is presented in Figure 3.

As shown in Figure 3, each construction activity corresponds to an individual code. The first layer of individual coding is the construction activity list, which uses priority relationships to determine the order of construction activities. The second and third layers represent the construction plans and resources for each activity, respectively. As there is no sequential constraint on the plans and resources during the construction process, the population

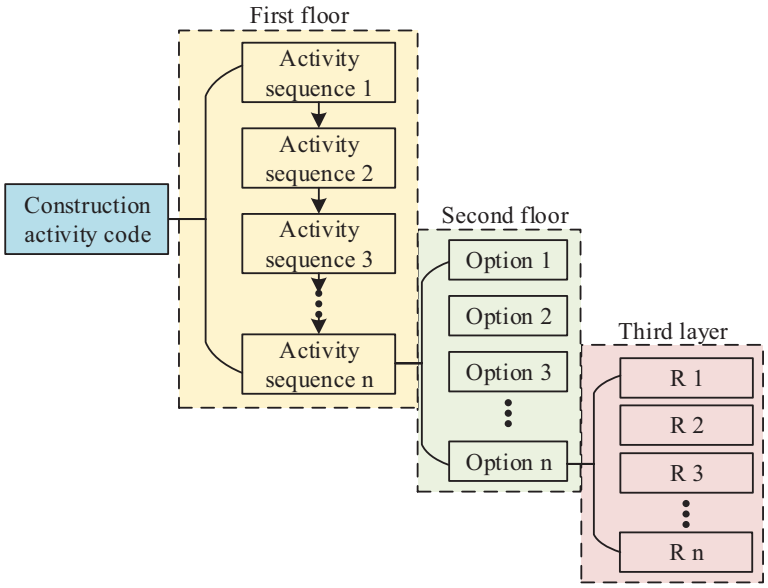

Figure 3 Design coding for decarbonization and emission reduction in buildings based on NSGA-II algorithm.

individuals representing the construction plans and resources are initialized randomly. Through this encoding method, the NSGA-II algorithm can automatically adjust the order, scheme, and resources of various construction activities during the optimization process, thereby achieving comprehensive optimization of multiple objectives such as CEs, construction period, and cost. The objective function of the general NSGA-II algorithm often adopts abstract mathematical expressions, while the multi-objective function in this study is completely based on the carbon emission data of the entire lifecycle of buildings, and achieves dynamic data linkage with BIM models. The MOO model is presented in Equation (7).

$$\begin{cases} \min E = \sum_{i=1}^{n} \sum_{j=1}^{m} (Q_r^{ij} \times F_r^{ij}) \\ \min T = \sum_{i=1}^{n} \sum_{j=1}^{m} (Q_r^{ij} \times H_r^{ij}) \\ \min W = \sum_{i=1}^{n} \sum_{j=1}^{m} (Q_r^{ij} \times P_r^{ij}) \end{cases} \tag{7}$$

In Equation (7), E, T, and W represent CEs, construction period, and cost. H_r^{ij} and P_r^{ij} represent the planned time and unit cost of the ith project in the jth construction plan. The computation for the duration objective function is presented in Equation (8).

$$\min T = \sum_{i=1}^{n} T_i = \sum_{i=1}^{n} \sum_{j=1}^{m} I_r^{ij} = \sum_{i=1}^{n} \sum_{j=1}^{m} (Q_r^{ij} \times H_r^{ij}) \tag{8}$$

In Equation (8), T_i is the construction time of the ith project, and I_r^{ij} is the construction time of the rth item in the ith project under the jth construction plan. The computation for the cost objective function is presented in Equation (9).

$$\min W = \sum_{i=1}^{n} W_i = \sum_{i=1}^{n} \sum_{j=1}^{m} S_r^{ij} = \sum_{i=1}^{n} \sum_{j=1}^{m} (Q_r^{ij} \times P_r^{ij}) \tag{9}$$

In Equation (9), W_i is the total cost of the ith construction project, and S_r^{ij} is the cost of the jth item in the ith project under the rth construction plan [14]. The computation for unit cost is presented in Equation (10).

$$P_r^{ij} = U_r^{ij} + V_r^{ij} + K_r^{ij} \tag{10}$$

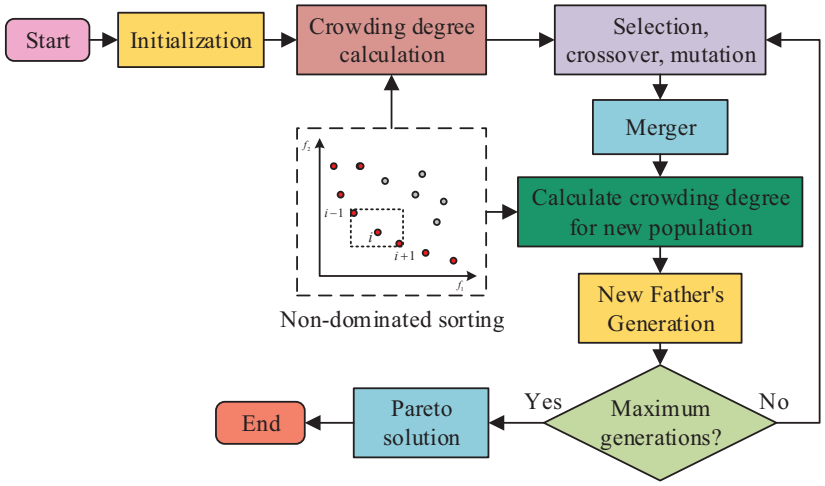

Figure 4 Zero carbon buildings decarbonization and emission reduction process based on NSGA-II MOO.

In Equation (10), U_r^{ij}, V_r^{ij}, and K_r^{ij} indicate the material, labor, and machinery costs for the jth project in the ith project under the rth construction plan. In addition, the constraints of the above-mentioned objective function are set as follows. Resource constraints require that the usage of labor, mechanical equipment and key materials for each type of work does not exceed the total available amount. The construction period constraint requires that the total construction period must not exceed the latest completion time stipulated in the contract. Cost constraints require that the total cost be controlled within the budget range. Carbon emission constraints require that the carbon emissions at each stage do not exceed the local environmental protection policy limits. The decarbonization and emission reduction process of zero carbon buildings based on NSGA-II MOO is presented in Figure 4.

As shown in Figure 4, in this process, the system first initializes the construction plan with a population and subsequently conducts non-dominated sorting and congestion calculation on the initial population. Then, it generates a new generation of subgroups through selection, crossover, mutation, and other operations, and merges the parent and offspring generations. At this stage, the system performs fast non-dominated sorting and crowding calculation on the new population and selects appropriate members to create a new parental generation. Next, it determines whether the maximum evolutionary number has been attained. If the number has not been reached, the system

repeats the generation of subgroups and subsequent operations. If the number has been reached, it obtains a Pareto frontier solution. Finally, the system selects a solution based on the three objectives of CEs, cost, and project duration. The study used the roulette wheel method to select parent individuals, and the individual's selection probability is presented in Equation (11).

$$P_i = \frac{f_i}{\sum_{i=1}^{N} f_i} \tag{11}$$

In Equation (11), P_i is the probability of individual i being selected, N is the population size, and f_i is the fitness of individual i. The population crossover process is presented in Equation (12).

$$\begin{cases} a_{ij} = a_{ij}(1-\alpha) + a_i\alpha \\ a_{ij} = a_{ij}(1-\alpha) + a_{ij}\alpha \end{cases} \tag{12}$$

In Equation (12), a_{ij} is the chromosome of individual i, and α is a number chosen at random within the range of 0 to 1. The mutation operation process is presented in Equation (13).

$$\begin{cases} a_{ij} + (a_{ij} - a_{max}) \times f(g), & \beta > 0.5 \\ a_{ij} + (a_{\min} - a_{ij}) \times f(g), & \beta \leq 0.5 \end{cases} \tag{13}$$

In Equation (13), $a_{\max}$ and $a_{\min}$ represent the max and min values of the chromosome in individual i, $f(g)$ is the mutation factor, and β is a number chosen at random within the range of 0 to 1. The computation of congestion is presented in Equation (14).

$$P(i)_{\text{distance}} = \sum_{k=1}^{r} [P(i+1) \cdot f_k - P(i-1) \cdot f_k] \tag{14}$$

In Equation (14), $P(i)_{\text{distance}}$ is the crowding distance of individual i, f_k is the value of the objective function k, r is the total number of objective function, $P(i+1)$ and $P(i-1)$ represent the adjacent solutions of individual i. To systematically evaluate the performance of the carbon emission model constructed in this study, the mean absolute percentage error (MAPE) and the full life cycle coverage were adopted as the core validation indicators. The error calculation is strictly based on the measured data of similar buildings in the MEIC database. The calculation method of MAPE is as shown in

Equation (15).

$$MAPE = \frac{1}{n \times m} \sum_{i=1}^{n} \sum_{j=1}^{m} \left| \frac{Y_{ij} - \widehat{Y}_{ij}}{Y_{ij}} \right| \times 100\% \tag{15}$$

In Equation (15), $MAPE$ represents the average error, n represents the number of building samples in the MEIC database that match the research case, m represents the number of core sub types of carbon emissions throughout the lifecycle of the building, Y_{ij} represents the true carbon emissions of the j-th sub item in the i-th sample, and $\widehat{Y}_{ij}$ represents the predicted carbon emissions of the j-th sub item in the i-th sample. In the data preprocessing stage, multiple interpolation methods are used to supplement the missing values in the MEIC database, and Winsorize the extreme values to improve the data quality. The formula for calculating the full lifecycle coverage is shown in Equation (16).

$$P_C = \frac{S_{\text{covered}}}{S_{\text{total}}} \times 100\% \tag{16}$$

In Equation (16), P_C represents the coverage rate of the entire lifecycle, S_{covered} represents the total emissions corresponding to the core carbon emission sources covered by the model, and S_{total} represents the total emissions of all potential carbon emission sources throughout the lifecycle of the building. The evaluation criteria are as follows: A MAPE below 10% is generally considered to have good prediction accuracy of the model, and a MAPE below 5% is regarded as excellent. A coverage rate higher than 80% indicates that the model has a relatively complete coverage capacity for carbon emissions throughout the entire life cycle. The input data of the general NSGA-II algorithm relies heavily on manual sorting and input, which can lead to data lag or omission.

2 Analysis of Decarbonization and Emission Reduction Effects in Zero Carbon Buildings

2.1 Model Performance Analysis

To verify the capability of the model, an experimental environment was first set up. The experiment was based on the Ubuntu 16.04.7 LTS operating system, equipped with 128GB DDR4 RAM, RTX A5000 GPU, and using a 4TB NVMe SSD RAID 0+20TB HDD storage system. Meanwhile, modeling

was carried out using Autodesk Revit 2023 combined with Dynamo 2.13's BIM platform, and the optimization process was carried out using MATLAB R2022b software. The database used MySQL 8.0 and employed two publicly available datasets, MEIC and GCB. After preprocessing operations such as supplementation and cleaning on the basis of the original data, these datasets were categorized into training and testing sets in an 8:2 ratio. The public website for the MEIC dataset is: http://www.meicmodel.org/, the source of the GCB dataset is: https://www.globalcarbonproject.org/index.htm. Among them, the MEIC data is sourced from its public platform, covering the carbon emission factors and construction-related activity levels by province and industry in China from 2018 to 2022. The GCB data is sourced from the official website of the Global Carbon Initiative and includes global and major national energy-related CO_2 emissions and carbon sink data from 1960 to 2022. The data processing is as follows: Firstly, the MEIC data is screened to extract the emission categories related to the construction industry, and then mapped and matched with the material, energy and process data in the BIM model. At the same time, based on the historical trend of GCB and the shared socio-economic path scenario, two emission scenarios, namely "standard operation" and "low-carbon energy allocation", are constructed, and global data is regionally adapted according to the proportion of China's energy structure. Missing values are interpolated using the mean of similar data, and outliers are truncated by ± 3 times the standard deviation. Finally, the organized data is divided into a training set and a test set in an 8:2 ratio for model training and independent validation. The algorithm's population was configured with a size of 100, while the crossover and mutation rates were established at 0.9 and 0.1, respectively. Set the evolutionary algebra to 200 to ensure the algorithm converges fully. Cross-operation only involves the exchange of plans and resources within the same construction activity. Mutation operations allow for random adjustments to the sequence of activities, changes to construction plans or resource types within the scope of compliance. Constraint processing adopts the constraint-Domination Principle, placing the infeasible solutions at a lower ranking level to guide the population to evolve towards the feasible domain. Detailed information about the experimental setup can be found in Table 1.

It can be known from Table 1 that the selection of software versions is based on its stability, functional compatibility and industry-wide applicability. Ubuntu 16.04.7 LTS is the long-term supported version, which is stable and compatible with most scientific computing libraries. Autodesk Revit 2023 supports complete export of BIM data and Dynamo 2.13 visual

Table 1 Experimental environment configuration

Environment	Configuration
Operating system	Ubuntu 16.04.7 LTS
CPU	Intel Core i7-9700
GPU	NVIDIA RTX A5000
Memory	128GB DDR4 RAM
Storage system	4TB NVMe SSD RAID 0 + 20TB HDD
BIM modeling platform	Autodesk Revit 2023 + Dynamo 2.13
Optimization software	MATLAB R2022b
Database	MySQL 8.0

programming. MATLAB R2022b provides a mature toolkit of optimization algorithms and support for parallel computing; MySQL 8.0 performs exceptionally well in data query and transaction processing efficiency. The hardware configuration is mainly aimed at computationally intensive tasks such as BIM model processing, NSGA-II large-scale population iteration, and database parallel query, ensuring that the model is trained and optimized within a reasonable time. The research case was a building that adopted a multi-layer framework structure. The design life of the building was 50 years, with a total construction area of 3742.6 m^2, a land area of 753.69 m^2, a total building height of 18.4 m, and a total of 5 floors. Due to the large footprint, complex construction, and high material consumption of this building project, a substantial quantity of CEs was generated during the construction process. To verify the capability of the proposed model, construction data of the project was collected and a BIM model was constructed. The Pareto solution of the multi-objective model studied is presented in Figure 5. From Figure 5(a), the model studied in the training set successfully provided 8 Pareto solutions. Among them, the optimal solution had a CE of 105.64 tons, corresponding to a construction period of 253 days and a cost of 9.57 million yuan. The worst-case scenario for CEs was 751.67 tons, with a construction period of 479 days and a cost of 16.72 million yuan. From Figure 5(b), the Pareto solution scheme was also successfully provided in the test set.

The reason why the population size is set to 100 but only generates 8 sets of solutions is that this is a natural result of the core mechanism of NSGA-II algorithm, non dominated sorting. The initial 100 individuals need to go through multiple rounds of selection, crossover, and mutation iterations. In each iteration, most individuals are eliminated due to being dominated, while only non dominated individuals are retained, ultimately forming 8 sets of non dominated Pareto solutions. This is not an algorithmic flaw, but

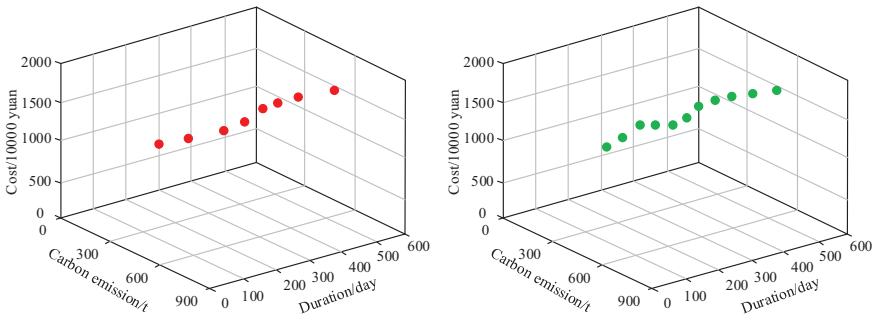

(a) Pareto solutions in the training set

(b) Pareto solutions in the test set

Figure 5 Pareto solution of multi-objective model.

a reflection of the algorithm's ability to select the truly optimal trade-off solution. The reason why the three objectives that do not converge are not directly merged is that convergence here refers to the gradual stabilization of each objective within a reasonable range as the number of iterations increases, rather than the convergence of the three objectives to the same value or becoming interchangeable with each other. Each of the 8 Pareto solutions represents a unique trade-off relationship. If these solutions are merged, the diversity of trade-off schemes will be lost and they will not be able to adapt to different engineering scenarios. The study adopts a dual criteria approach of non dominated sorting combined with crowding distance calculation, which is a recognized scientific method in the field of multi-objective optimization. Among them, non dominated sorting divides individuals into different ranks based on their dominance relationships, with individuals with lower ranks being superior to those with higher ranks because the former is not dominated by any other individuals. The calculation of crowding distance is for individuals of the same non dominated level. The crowding distance reflects the sparsity of the individual in the solution set. The larger the crowding distance, the lower the similarity between the individual and adjacent solutions, providing a more unique trade-off solution. Therefore, when selecting the final solution from 8 sets of Pareto solutions based on the above dual criteria, decision-makers can prioritize individuals with larger crowding distances to ensure that the selected solution covers the most valuable trade-off scenarios, rather than relying on subjective judgments. The final selection process of Pareto front based on TOPSIS method is as follows: first, clarify the decision attributes and weight allocation, then standardize the Pareto solution data, and determine the positive ideal solution and negative ideal solution based on

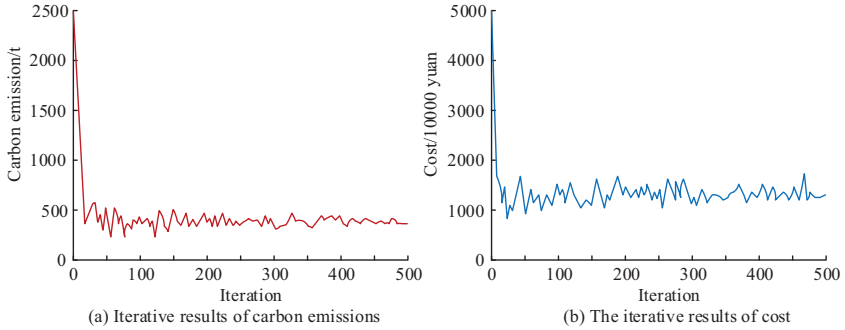

Figure 6 Iterative results of CEs and costs.

this. Then, calculate the weighted Euclidean distance between each solution and the ideal solution, and calculate the comprehensive closeness. Sort and select the optimal solution based on the size of the comprehensive closeness. From the above, the zero carbon building CE modeling method based on BIM technology was feasible and successfully obtained an MOO solution.

To verify the rationality of the decision-making scheme, a computer algorithm was introduced to iteratively calculate by assigning different weights to the indicators of CEs and cost. The iterative results of CEs and costs are presented in Figure 6. From Figure 6, as the iteration count increased, the two indicators of CEs and cost gradually converged to a stable optimization result. This indicated that the model had good convergence and optimization effects, and could effectively solve the balance optimization problem between CEs and costs.

To further assess the model's effectiveness, it was benchmarked against other common CE models, including the Model from the China Energy and CE Database (MEIC), Long range Energy Alternatives Planning System Model (LEAP), and Economic Input Output Life Cycle Assessment Model (EIO-LCA) [15–17]. Figure 7 illustrates how various models performed when evaluated on the MEIC dataset. From Figure 7(a), under the training set, the average error rate of the MOO model studied was only 4.20%. Compared with the average error rates of models such as MEIC, LEAP, and EIO-LCA, which were 6.57%, 5.82%, and 7.35%, they decreased by 2.37%, 1.62%, and 3.15%. The lifecycle coverage of the research model was as high as 87.92%, while the coverage of other models was 80.45%, 85.10%, and 75.69%. The research model improved by 7.47%, 2.82%, and 12.23% compared to them. From Figure 7(b), in the test set, the average error rate and lifecycle coverage of the research model were 4.15% and 88.23%, which were also better

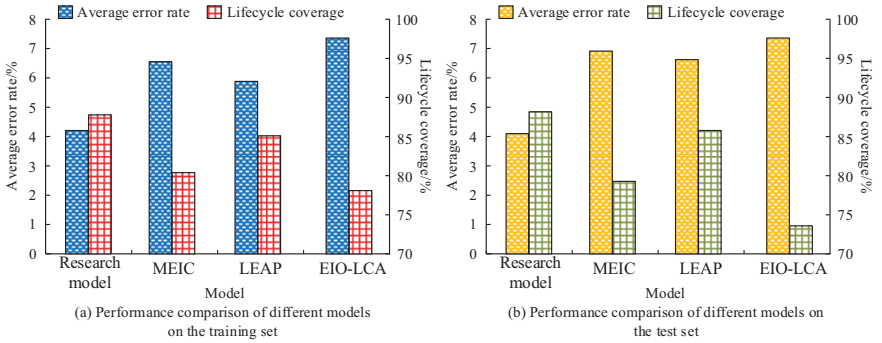

Figure 7 Performance comparison of various models on the MEIC dataset.

Table 2 Performance comparison of various models on the training and testing sets

Data Set	Index	Research Model	MEIC	LEAP	EIO-LCA
Training set	Training time/h	3.48	5.72	4.21	6.15
	Inference time/s	0.02	0.18	0.12	0.16
	R^2	0.93	0.84	0.86	0.79
	MSE	0.0028	0.0094	0.0076	0.0132
Test set	Training time/h	3.51	5.12	4.24	6.04
	Inference time/s	0.02	0.15	0.08	0.12
	R^2	0.92	0.85	0.88	0.80
	MSE	0.0025	0.0085	0.0064	0.0127

than other models. In summary, the MOO model based on BIM technology showed significant advantages in the accuracy and lifecycle coverage of CE prediction.

To comprehensively verify the performance of the model, the study compared the performance of various models on the training and testing sets, as shown in Table 2. From Table 2, the performance of the research model was significantly better than other models on both the training and testing sets. In regard to computational efficiency in the test set, the training time for the research model was only 3.51 hours, while the training time for other models was all over 4 hours. In addition, its inference time only took 0.02 seconds. Although other models had shorter inference times, the research model still had significant advantages, demonstrating its superior computational performance and deployment adaptability. In terms of fitting accuracy, the determination coefficient R2 of the research model was as high as 0.92, which was 8.23%, 4.54%, and 15% higher than the determination coefficients of models such as MEIC, LEAP, and EIO-LCA. In terms of

generalization ability, the mean squared error (MSE) of the research model was only 0.0025, which was 70.58%, 60.93%, and 80.31% lower than the other three models. In summary, MOO models based on BIM technology had superior performance in CE modeling applications.

2.2 Analysis of Emission Reduction Effects

To verify the energy-saving and emission reduction effects of the MOO model scheme based on BIM technology, this study compared the CE data of the optimized scheme and the unoptimized scheme, evaluated the CE reduction effects of the optimized scheme at different stages, and verified the CE reduction effects throughout the whole span and operation stages. The experimental group used the optimization scheme in the MOO model for comprehensive CE monitoring, while the control group used the unoptimized traditional scheme for CE monitoring. GCB data were used to simulate the CEs of unoptimized and optimized schemes.

The comparison of emission reduction effects before and after optimization is presented in Figure 8. From Figure 8(a), under standard operating conditions, the optimized scheme had a CEs of 2108.51 tons throughout its whole span, a reduction of 35.06% compared to the pre optimization level of 3246.94 tons. The CEs during the operation phase of the optimized plan were 1193.95 tons, a reduction of 43.69% compared to 2120.69 tons before optimization. From Figure 8(b), under the condition of low-carbon energy allocation, the optimized scheme had a CE of 1786.83 tons throughout its whole span, which was a 44.96% reduction compared to the pre optimized 3246.82 tons. The CEs during the operation phase of the optimized plan were 1097.52 tons, a reduction of 47.93% compared to 2108.13 tons before optimization. From Figure 8(c), under standard operating conditions, the energy consumption of the optimized and non optimized schemes was 2561.87 MWh and 1489.62 MWh, a reduction of 41.85%. Meanwhile, the CE intensity before and after optimization were 0.18 $kgCO_2$/kWh and 0.12 $kgCO_2$/kWh, respectively, a decrease of 33.33%. From Figure 8(d), under the condition of low-carbon energy allocation, the energy consumption of the optimized and non optimized schemes were 2397.08 MWh and 1328.54 MWh, a reduction of 44.57%. The CE intensity before and after optimization were 0.16 $kgCO_2$/kWh and 0.11 $kgCO_2$/kWh, a decrease of 31.25%. In summary, the research method effectively reduced energy consumption and CE intensity. In summary, the research method achieved significant carbon reduction effects in different scenarios.

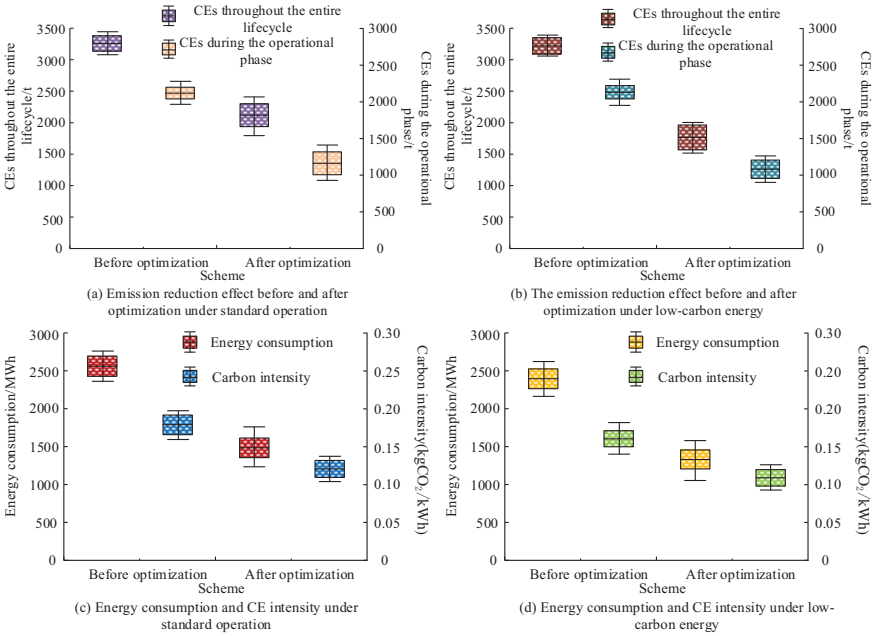

Figure 8 Comparison of emission reduction effects before and after optimization of the plan (a) Under standard operating conditions, the optimized carbon emissions throughout the entire lifecycle are reduced by 35.06%, and during the operational phase, they are reduced by 43.69%; (b) Under the conditions of low-carbon energy allocation, the optimized carbon emissions throughout the entire lifecycle are reduced by 44.96%, and the operational phase is reduced by 47.93%; (c) Under standard operating conditions, energy consumption decreased by 41.85% and carbon intensity decreased by 33.33%; (d) Under low-carbon energy allocation conditions, energy consumption decreased by 44.57% and carbon intensity decreased by 31.25%.

The specific measures for achieving zero carbon are as follows: 1. For the core energy load during the operation phase of the building, a distributed photovoltaic combined with energy storage system is configured to achieve zero carbon substitution of electricity consumption. 2. For the remaining carbon emissions that cannot be further reduced through technological means during the construction and retirement phases, they will be offset by purchasing nationally certified voluntary emission reductions (CCERs). 3. Incorporate the full lifecycle emission reduction of buildings into the local carbon market, and form an economic guarantee mechanism for zero carbon targets through quota surplus trading combined with emission reduction pledge. In summary, zero carbon is not an absolute absence of carbon, but a net carbon of zero

throughout the entire lifecycle. Therefore, it requires a three-layer system of technological emission reduction, carbon offsetting and offsetting, and carbon market sustainability to achieve.

From this, it can be known that this result is highly representative in the following situations. First, the building type is actually applicable to medium-scale and medium-complexity public buildings, whose structural and energy system characteristics are similar to those of schools, office buildings, community centers and other types of buildings. For special types such as super high-rise buildings, industrial plants or historically protected buildings, parameter adjustments need to be made based on their structural systems, material usage and energy consumption patterns. The second factor is the influence of regional climate and energy structure. If it is applied in the extremely cold northern regions or the hot southern regions, the performance of the enclosure structure and the energy efficiency parameters of the equipment should be adjusted in combination with local climate data. In addition, the carbon intensity of regional power grids directly affects the carbon emissions during operation. In application, the carbon emission factors need to be updated based on the local energy structure. The third aspect is the portability of emission reduction measures. The emission reduction measures studied and adopted, such as distributed photovoltaic + energy storage, high-efficiency envelope structures, and construction process optimization, have good universality. However, the specific implementation effects will be affected by local resource conditions, such as sunshine hours, the origin of building materials, construction technology levels, and policy environments. Therefore, it is recommended that when promoting and applying it, the model be calibrated in combination with the type characteristics of the target building, regional climate, energy structure and local carbon emission factors to ensure the accuracy and applicability of emission reduction predictions.

To confirm the MOO effect of the model, the CE reduction effects under different optimization schemes were compared and studied, as shown in Table 3. From Table 3, the MOO scheme in the study reduced the project duration by 12.08%, cost by 0.91%, and CEs by 5.09% compared to the original scheme. This indicated that the plan has achieved an ideal balance between project duration, cost, and CEs. Compared to this, although the single objective optimization plan for construction period shortened the construction period by 18.12%, the cost increased by 4.73%, and the CEs also increased by 2.65%. The cost reduction of the cost single objective optimization plan was 9.01%, but its construction period was only reduced by 2.68%, and CEs were only reduced by 2.78%. In the single objective optimization

Table 3 Comparison of CE reduction effects under different optimization schemes

Optimization Plan	Duration/ Day	Change Rate of Construction Period/%	Cost/ 10000 Yuan	Cost Change Rate/%	CE/t	CE Change Rate/%
Original scheme	149	/	2205.67	/	10805.69	/
MOOn	131	−12.08%	2185.64	−0.91%	10254.25	−5.09%
Single objective optimization of construction period	122	−18.12%	2309.92	4.73%	11091.08	2.65%
Cost target optimization	145	−2.68%	2009.41	−9.01%	10504.16	−2.78%
Optimization of CE Single Target	137	−8.05%	2155.93	−2.26%	10263.28	−5.00%

scheme for CEs, although CEs were reduced by 5.00%, the construction period and cost were only reduced by 8.05% and 2.26% respectively, both of which were lower than the effect of the MOO scheme. In summary, the MOO method studied could effectively improve overall efficiency and successfully achieve a balance between project duration, cost, and CEs.

3 Discussions

With the increasing importance of global low-carbon development and green energy conservation, carbon reduction has emerged as a major focus for nations globally. Therefore, to promote decarbonization, emission reduction, and low-carbon energy applications, a zero carbon building CE management method based on full lifecycle CE modeling and MOO was proposed. The outcomes revealed that the decarbonization and emission reduction scheme for zero carbon buildings based on MOO successfully provided 8 Pareto solutions, providing feasible solutions for the optimization design of CE reduction schemes for zero carbon buildings.

The innovation core of the research is not the invention of new algorithms, but rather the scenario based transformation and cross technology integration of mature algorithms around the optimization of carbon emissions throughout the life cycle of zero carbon buildings. The three innovative points of three-layer coding logic, BIM linkage objective function, and data optimization closed-loop have solved the problems of infeasible solutions and data fragmentation in the application of the general NSGA-II algorithm in the field of buildings. In addition, the study innovatively constructed

an integrated method system combining BIM modeling and dual database verification. BIM technology achieves full lifecycle data integration, the modified NSGA-II algorithm achieves multi-objective collaborative optimization, MEIC database verifies model accuracy, and GCB database predicts multi scenario emission reduction effects. This systematic innovation is not limited to the use of the NSGA-II algorithm alone, and can effectively support engineering feasibility.

From the perspective of model performance, the average error rate of the MOO model proposed in the study was 4.20%, while other models were all greater than 5%, indicating that this model had a significant advantage in the accuracy of CE calculation. Furthermore, the lifecycle coverage of the research model was as high as 87.92%, which could more comprehensively cover the CEs of the whole span of the building. This was because the research was based on models constructed using BIM technology. Safikhani S et al.'s research also confirmed that BIM technology could achieve coverage of information in various stages of engineering by integrating data from the whole span [18]. In terms of computational efficiency and fitting accuracy, the training time of the research model in the test set was only 3.51 h, and the inference time only took 0.02 s. Compared with other models with training time of more than 4 h, it was more conducive to practical deployment and application. Furthermore, in regard to fitting accuracy, the determination coefficient R^2 of the research model was as high as 0.92, which was more than 5% higher than other models, indicating that the model had a better fitting effect on the data. In terms of generalization ability, the MSE of the research model was only 0.0025, reflecting a stronger ability to adapt to different scenarios. Disney O et al.'s research also confirmed the efficiency and stability of BIM technology in data processing in the field of architecture [19].

From the perspective of emission reduction effect, the optimization plan achieved significant emission reduction and energy conservation effects under both standard operating conditions and low-carbon energy allocation conditions. Under standard operating conditions, the optimization plan resulted in a 35.06% reduction in CEs throughout the whole span compared to before optimization. Under low-carbon energy allocation conditions, CEs were reduced by 44.96%. This indicated that the optimization plan could effectively reduce CEs throughout the whole span, with a reduction rate between 35% and 45%. In addition, compared to the original plan, the optimized plan reduced the construction period by 12.08%, cost by 0.91%, and CEs by 5.09%. This indicated that the plan achieved an ideal balance between project duration, cost, and CEs. This was because the study used

the NSGA-II algorithm for MOO. The study by Canbolat A S et al. also confirmed that such algorithms could find the optimal solution to balance various objectives under multiple constraint conditions [20].

In summary, the zero carbon building lifecycle CE modeling and MOO method studied showed excellent performance in model performance, computational efficiency, and optimization effects.

4 Conclusion

With the increasing demand for low-carbon development worldwide, carbon reduction has become an important goal in promoting energy transition. Therefore, modeling and MOO analysis were conducted on the CEs throughout the whole span of zero carbon buildings. The outcomes revealed that the average error rate of the research model was 4.20%, which was 2.37%–3.15% lower than other models. The lifecycle coverage reached 87.92%, an increase of 2.82%–12.23% compared to other models. In terms of computational efficiency, the training time of the research model was 3.51 h, and the inference time was only 0.02 s, both significantly better than other models. In addition, the R^2 of the model was as high as 0.92, and the MSE was only 0.0025, indicating its excellent model performance. From the perspective of emission reduction effect, the optimization plan achieved a 35.06% reduction in CEs throughout the whole span under standard operating conditions, while under low-carbon energy allocation conditions, the reduction rate reached 44.96%. Meanwhile, the optimized plan reduced energy consumption and CE intensity by 41.85% and 33.33% respectively under standard operating conditions, indicating that the optimized plan achieved an ideal balance between schedule, cost, and CEs. In summary, the zero carbon building whole span CE modeling and MOO method studied effectively achieved energy conservation and emission reduction. However, in the modeling process, the research mainly focuses on core projects and materials with high carbon emissions, such as steel, concrete, construction machinery, etc., and does not conduct detailed calculations for projects and materials with low carbon emissions, such as some decorative materials, auxiliary processes, etc. However, due to the relatively low proportion of low-carbon projects in total carbon emissions, usually less than 10%, their impact on the overall emission reduction conclusion is limited. Future research can further introduce a carbon emission grading accounting mechanism to classify and refine calculations for high, medium, and low-carbon emission projects, and explore the coupled emission reduction effects of low-carbon technologies throughout their entire lifecycle,

in order to improve the completeness and accuracy of the model's evaluation of zero carbon technologies.

Declaration of Conflict

The author declares no conflicts of interest.

Author Contributions Statement

Xueli Yin and Yingrui Dong wrote the main manuscript text and Rong Hu and Luyao Pei prepared figures. All authors reviewed the manuscript.

Funding

None.

Consent to Publish Declaration

Not applicable.

Ethics and Consent to Participate declarations

Not applicable.

References

[1] Wang W, Tang Q, Gao B. Exploration of CO_2 emission reduction pathways: identification of influencing factors of CO_2 emission and CO_2 emission reduction potential of power industry. Clean Technologies and Environmental Policy, 2023, 25(5): 1589–1603. https://doi.org/10.1007/s10098-022-02456-1.

[2] Wu X, Xu C, Ma T, Xu J, and Zhang C. Carbon emission of China's power industry: driving factors and emission reduction path. Environmental Science and Pollution Research, 2022, 29(52): 78345–78360. https://doi.org/10.1007/s11356-022-21297-5.

[3] Watari T, Yamashita N, Serrenho A C. Net-Zero Embodied Carbon in Buildings with Today's Available Technologies. Environmental Science And Technology, 2024, 58(4): 1793–1801. https://doi.org/10.1021/acs.est.3c04618.

[4] Yu K, van Son P. Review of trans-Mediterranean power grid interconnection: A regional roadmap towards energy sector decarbonization. Global Energy Interconnection, 2023, 6(1): 115–126. https://doi.org/10.1016/j.gloei.2023.02.010.

[5] Roijen E V, Miller S A, Davis S J. Building materials could store more than 16 billion tonnes of CO_2 annually. Science, 2025, 387(6730): 176–182. https://doi.org/10.1126/science.adq8594.

[6] Liu J, Ma H, Wang Q, Tian, S., Xu, Y., Zhang, Y, and Yang, S. Optimization of energy consumption structure based on carbon emission reduction target: A case study in Shandong Province, China. Chinese Journal of Population, Resources and Environment, 2022, 20(2): 125–135. https://doi.org/10.1016/j.cjpre.2022.06.003.

[7] Mullen D, Herraiz L, Gibbins J, and Lucquiaud M. On the cost of zero carbon hydrogen: A techno-economic analysis of steam methane reforming with carbon capture and storage. International Journal of Greenhouse Gas Control, 2023, 126(c): 103904–103904. https://doi.org/10.1016/j.ijggc.2023.103904.

[8] Li H, Hao T, Li Z, Zhao, E., Wang, C & Xu, L. Research on a self-coordinated optimization method for distributed energy resources targeting risk mitigation. Distributed Generation and Alternative Energy Journal, 2024, 39(3): 659–690. https://doi.Org/10.13052/dgaej2156-3306.39312.

[9] Shu Y, Zhang L, Zhang Y, Wang, Y., Lu, G., Yuan, B. Carbon peak and carbon neutrality path for China's power industry. Strategic Study of Chinese Academy of Engineering, 2021, 23(6): 1–14. https://doi.org/10.15302/J-SSCAE-2021.06.001.

[10] Ding C, Ke J, Levine M, Granderson, J. and Zhou, N. Potential of artificial intelligence in reducing energy and carbon emissions of commercial buildings at scale. Nature Communications, 2024, 15(1): 5916–5920. https://doi.org/10.1038/s41467-024-50088-4.

[11] Zhuo Z, Du E, Zhang N, Nielsen, C. P., Lu, X., Kang, C. Cost increase in the electricity supply to achieve carbon neutrality in China. Nature communications, 2022, 13(1): 3172–3180. https://doi.org/10.1038/s41467-022-30747-0.

[12] Cheng D, Reiner D M, Yang F, Cui, C., Meng, J., Shan, Y & Guan, D. Projecting future carbon emissions from cement production in developing countries. Nature Communications, 2023, 14(1): 8213–8215. https://doi.org/10.1038/s41467-023-43660-x.

[13] Zhang S, Chen W. Assessing the energy transition in China towards carbon neutrality with a probabilistic framework. Nature communications, 2022, 13(1): 87–95. https://doi.org/10.1038/s41467-021-27671-0.

[14] Bistline J E T, Blanford G J. Impact of carbon dioxide removal technologies on deep decarbonization of the electric power sector. Nature Communications, 2021, 12(1): 3732–3741. https://doi.org/10.1038/s41467-021-23554-6.

[15] Liu Z, Deng Z, Davis S J, Giron, C., and Ciais, P. Monitoring global carbon emissions in 2021. Nature Reviews Earth & Environment, 2022, 3(4): 217–219. https://doi.org/10.1038/s43017-022-00285-w.

[16] Gao Z, Xie H, Yang X, Yang, X., Zhang, L., Yu, H., Wang, W and Chen, S. Electric vehicle lifecycle carbon emission reduction: A review. Carbon Neutralization, 2023, 2(5): 528–550. https://doi.org/10.1002/cnl2.81.

[17] Wang P, Lin C K, Wang Y, Liu, D., Song, D., and Wu, T. Location-specific co-benefits of carbon emissions reduction from coal-fired power plants in China. Nature communications, 2021, 12(1): 6948–6952. https://doi.org/10.1038/s41467-021-27252-1.

[18] Slameršak A, Kallis G, O'Neill D W. Energy requirements and carbon emissions for a low-carbon energy transition. Nature communications, 2022, 13(1): 6932–6937. https://doi.org/10.1038/s41467-022-33976-5.

[19] Disney O, Roupé M, Johansson M, and Domenico Leto, A. Embracing BIM in its totality: a Total BIM case study. Smart and Sustainable Built Environment, 2024, 13(3): 512–531. https://doi.Org/10.1108/SASBE-06-2022-0124.

[20] Canbolat A S, Albak E İ. Multi-Objective Optimization of Building Design Parameters for Cost Reduction and CO_2 Emission Control Using Four Different Algorithms. Applied Sciences, 2024, 14(17): 7668–7672. https://doi.org/10.3390/app14177668.

Biographies

Xueli Yin (1979.1–), female, graduated from Huazhong University of Science and Technology with a bachelor's degree in Electrical Engineering and Automation in 2002. In 2019, she joined China Southern Power Grid Energy Development Research Institute Co., Ltd. as a senior researcher. Her current research interests include AC and DC power transmission and transformation projects, as well as smart grid technology.

Yingrui Dong (1987.9–), male, graduated from South China University of Technology with a master's degree in Power Electronics and Electric Drive in 2012. In 2024, he joined China Southern Power Grid Energy Development Research Institute Co., Ltd. as a researcher. His current research interests lie in new energy generation and grid integration, as well as smart grid technology.

Luyao Pei (1989.02–), male, graduated from China University of Geosciences (Wuhan) with a master's degree in Geographic Information Systems in 2015. In 2020, he joined China Southern Power Grid Energy Development Research Institute Co., Ltd. as a researcher. His current research direction is power grid digital twins.

Rong Hu (1987.5–), female, graduated from Wuhan University with a master's degree in High Voltage and Insulation Technology in 2010. In 2023, she joined China Southern Power Grid Energy Development Research Institute Co., Ltd. as a researcher. Her current research interests include flexible DC transmission technology and the construction of green and low-carbon power grids.